Size-Selective 2D Ordering of Gold Nanoparticles Using Surface Topography of Self-Assembled Diamide Template

Neralagatta M. Sangeetha,* Christian Blanck, Thi Thanh Tam Nguyen, Christophe Contal, and Philippe J. Mésini

Institut Charles Sadron, 23 rue du Loess, BP 84037, 67034 Strasbourg Cedex 2, France

ABSTRACT

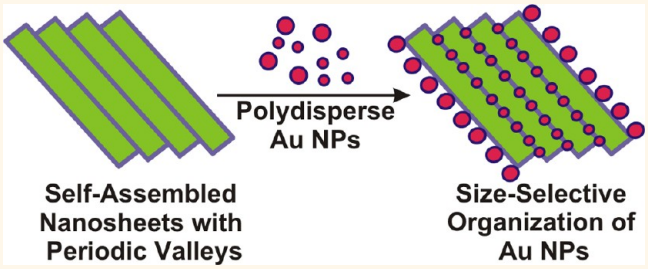

Size-selective organization of ~2 nm dodecanethiol stabilized gold nanoparticles (AuNPs) into periodic 1D arrays by using the surface topographical features of a soft template is described. The template consists of micrometer length nanotapes organized into nanosheets with periodic valleys running along their length and is generated by the hierarchical self-assembly of a diamide molecule (BHPB) in cyclohexane. The AuNP ordering achieved simply by mixing the preformed template with the readily available ~2 nm dodecanethiol stabilized AuNPs is comparable to those obtained using programmable DNA and functional block copolymers. The observed periodicity of the AuNP arrays provided valuable structural clues about the organization of nanotapes into nanosheets. Self-assembling BHPB molecules in the presence of AuNPs by heating and cooling the two components led to a comparatively disordered organization because the template structure was changed under these conditions. Moreover, the template could not order larger AuNPs (~5 nm) into a similar 1D array, owing to the steric restriction imposed by the dimension of the valleys on the template. Interestingly, this geometric constraint led to AuNP size sorting when a polydisperse sample (2.5 ± 0.9 nm) was used for organization, with AuNPs attached to the template edges being larger (≥2.2 ± 0.9 nm) than those associated to the inner valleys (1.6 ± 0.8 nm). This is a unique example of size-sorting induced by the surface topographical features of a soft template.

KEYWORDS: self-assembly · nanotapes · nanosheets · gold nanoparticles · 1D arrays · size-selection · size-sorting

Organizing nanoscale building blocks into well-defined architectures is one of the intensely pursued topics of nanotechnology.[1−4] This is of significance not only for the design of nanodevices but also for the fundamental understanding of the collective properties arising from interparticle interactions within the assembly. Several physical and chemical strategies are being developed to obtain organized assemblies of nanomaterials.[5−9] One of the popular strategies involves the use of soft templates to guide nanoparticle organization.[8] Template directed assembly approaches make use of supramolecular interactions between appropriately modified nanoparticle (NP) surfaces and active sites of the template, to induce nanoparticle ordering. Three classes of polymeric materials, namely, biopolymers (DNA, RNA and proteins),[4,9−14] synthetic polymers (functional block copolymers),[15−18] and supramolecular polymers (self-assembled small molecules)[19−30] have been explored to this end. Among these, biopolymers and block polymers have been explored extensively for the purpose of spatially ordering NPs. For example, by tuning the interaction between the nanoparticles and the template, control over spatial arrangement of nanoparticles (2D or 3D) has been achieved using programmed DNA[13,14] and phase separating block copolymer templates.[16−18] These templates have also been used to obtain size-selective NP assemblies by implementing disparate interactive domains into their structures for enabling site-specific attachment of differently sized nanoparticles.[13,17] In comparison to this, progress in exploiting supramolecular polymers as templates has not been significant. Using these materials, NP organization has been controlled in only one direction,[19−30] as with certain linear polymeric structures.[31] A distinct advantage of using supramolecular polymers for templating is that their precursors, small self-assembling molecules, can be prepared easily in large quantities, and their structures can be readily tailored to produce an extensive library of molecules to generate templates with varied architectures and also functions. Moreover, these templates can be disassembled fairly easily by external stimuli such as heat, pH, and chemicals.[19] In this report we demonstrate

* Address correspondence to: sangeetha_nm@yahoo.co.in.

Received for review November 3, 2011 and accepted September 2, 2012.

Published online September 13, 2012
10.1021/nn302206h

Chart 1. Structure of BHPB

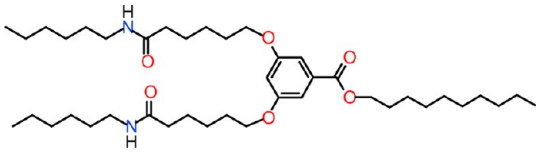

that supramolecular polymers can also serve as excellent templates for 2D organization of NPs. Significantly, the methodology utilized for NP organization is novel. The soft template used by us comprises micrometer length nanosheets self-assembled from a diamide molecule, BHPB (Chart 1) in cyclohexane.[32] These nanosheets present periodic nanovalleys running along their length, which not only facilitated the organization of readily available dodecanethiol stabilized ~2 nm sized gold nanoparticles (AuNP) into 1D array, but also induced size-selectivity. The organization occurs through nonspecific van der Waals interaction and is guided by the surface topography of the template structure. This is the first example demonstrating the influence of the surface topography in the association of a soft template with hard spherical NPs, in liquid phase.

During the course of the study, we also discovered that small gold NPs could serve as probes to investigate morphologies and structural features of low contrast self-assembled organic superstructures by transmission electron microscopy (TEM). The gold NPs organized on the templates provided an excellent contrast in TEM images, presenting much more detailed information about the self-assembled superstructures as compared to those obtained from metal shadowing. Such strategies could serve as complementary tools in obtaining supplementary details on self-assembled superstructures, and may be more generally used to investigate morphologies of organic materials by TEM.

RESULTS AND DISCUSSION

Hierarchical Self-Assembly of BHPB. BHPB self-assembles into nanotubes, 27 nm in diameter and ~3 nm in wall thickness at concentrations >2% w/v in cyclohexane, resulting in the formation of a gel.[32] BHPB molecules associate through the $\pi-\pi$ interaction of the benzene cores and the intermolecular H-bonding interaction between the amide linkages of the side arms, and the nanotube formation is believed to be a result of coiling of initially formed nanotapes. Indeed, at lower concentrations (between 0.01 and 0.05% w/v), a suspension comprising nanotapes of several micrometers length was obtained (Figure 1 and Supporting Information, Figure S1). These nanotapes exhibited a remarkable ordering as observed by TEM and atomic force microscopy (AFM). AFM images of the suspension drop-casted on freshly cleaved mica (Figure 1b and Supporting Information, Figure S1) indicated that the nanotapes were organized laterally to form nanosheets with regularly

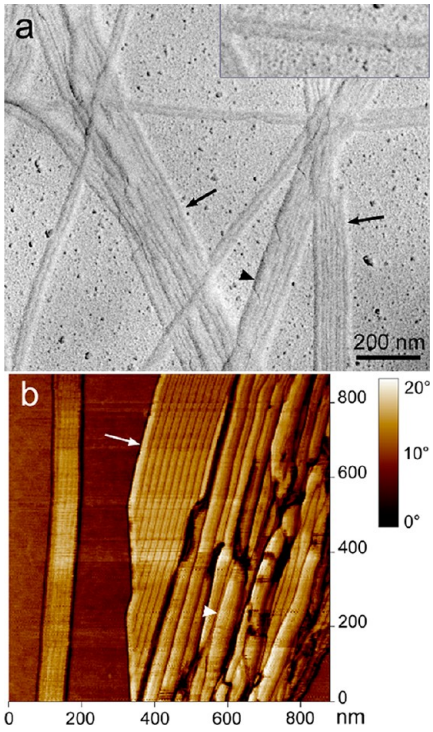

Figure 1. (a) TEM and (b) AFM phase images of self-assembled nanosheets of BHPB (0.02 wt % in cyclohexane) with the nanovalley feature: (Arrows) stacks of flat tapes arranged laterally to yield nanovalleys; (arrowhead) helical tape. Inset shows enlargement of twin tapes separated by a groove.

spaced valleys running parallel to their lengths. The number of nanotapes in the nanosheets ranged from 2 to about 30. AFM height analysis revealed that the nanotape thickness is about the length of BHPB (~3 nm) and that some of the laterally organized tapes are in turn stacked one on top of another. The width of an individual nanotape measured on TEM image is around 42 nm. This was in turn made up of two 21 nm units as indicated by a groove running parallel to this nanotape. Some twisted and coiled nanotapes coexisted with the organized nanotapes.

AuNP Organization. The BHPB nanosheets with nanovalleys running parallel to their length appeared to be promising templates for nanoparticle organization. For this, 1.7 $\pm$ 0.4 nm dodecanethiol stabilized AuNPs prepared by the Brust–Schiffrin strategy were used.[33] Among different methods that were tried for organizing AuNPs along the nanosheets, a simple mixing of the AuNPs with the prepared templates (mixing method) gave best results. Typically, AuNP organization could be achieved simply by mixing and shaking the suspension of BHPB nanotapes (0.02% w/v) and AuNP (0.002% w/v) in cyclohexane and letting the mixture stand overnight. The resulting mixture was dropcasted on carbon-coated copper grids supported on a filter paper to facilitate quick draining of the solvent, dried under ambient conditions, and observed by TEM without staining. Electron micrographs of the mixture (Figure 2a–c)

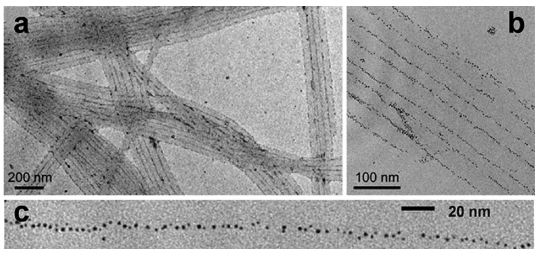

Figure 2. TEM images of AuNP arrays obtained by dropcasting a stabilized mixture of self-assembled nanosheets of BHPB (0.02% w/v) and 1.7 ± 0.4 nm dodecanethiol−AuNPs (0.002% w/v) in cyclohexane (mixing method), at different magnifications.

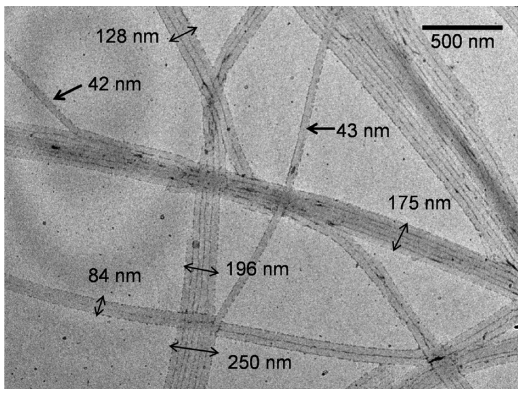

Figure 3. TEM image of AuNP arrays obtained by using the BHPB nanosheet template. The organization is directed by mono- and bilayered nanosheets and the measured widths of the templating superstructures are indicated.

indicated a highly ordered organization of NPs on the carbon-coated TEM grid: periodically spaced AuNP stripes ran several micrometers in length on the grids. When the observed morphology of the NP arrays was compared to that of BHPB nanotapes, it turned out that AuNPs are organized along the external edges and valleys of BHPB nanosheets. The internanoparticle distances within the stripes were mostly between 1.7 and 2.5 nm (Figure 2c). These values are less than twice the length of dodecanethiol molecule (1.52 nm), suggesting interdigitation of ligands between neighboring AuNPs.[34] Average distances between adjacent AuNP stripes were around 28, 35, or 42 nm. A distance of 7 nm was also measured mostly at the external edges. In addition, interstripe distances followed a pattern with the 28 nm distance never occurring at the external edges. Whereas the measured interstripe distance of 42 nm corresponds well with the measured width of an individual native BHPB nanotape, the presence of others (which are all multiples of 7) was intriguing. A rigorous analysis of the measured interstripe distances of the arrays formed by mono- and bilayered nanosheets indicated that this is due to overlapping of nanotapes in the nanosheets. Shown in Figure 3 are arrays of this type, where the measured widths of the nanosheets consisting of two, three, four, five and seven nanotapes are 84 (2 × 42), 128 (3 × 42), 154 (3.7 × 42), 196 (4.6 × 42) and 250 (6 × 42 nm), respectively. Not all these distances account for side-ways organization of nanotapes, as some are fractional multiples of 42 nm (width of a single nanotape). As the inter NP-stripe distance of a parallel pair of AuNP stripe which deviates from an array (corresponding to an individual nanotape) is always 42 nm, polydispersity in nanotape width is ruled out. Interestingly, all the inter NP-stripe distances measured are integer multiples of 7. This suggests that a 7 nm repeating unit is involved in the ordering of nanotapes. Using this piece of information, the observed inter NP-stripe distances can be attributed to the overlap of adjacent nanotapes in the nanosheets with a 7 nm offset. Evidence for this overlap was found in sections of TEM images where a nanosheet splits into two parts (Supporting Information, Figure S2).

A similar type of organization was observed when a 2-fold excess (0.004%) of AuNPs was used, with the AuNPs in excess largely remaining unattached to the template. In certain areas of the template, such as template edges and intersections at which two sheets cross each other, AuNP accumulation due to solvent drying effects was observed (Supporting Information, Figure S3). It is noteworthy that allowing a suspension of BHPB−AuNP mixtures on TEM grids to dry slowly does not result in the formation of linear arrays of AuNPs. TEM images of such samples show typical negative staining effect with the AuNPs accumulating around the edges of the template (Supporting Information, Figure S4). This is an indication that the observed AuNP organization is unlikely to have occurred on the TEM grids due to solvent drying effects.

Another method used for preparing the BHPB−AuNP hydrid is the self-assemby of the BHPB molecules in the presence of AuNPs (heat/cool method), a process commonly used for organizing NPs using self-assembled fibres.[20−25,27,28] In this method, a mixture of self-assembled BHPB (0.02% w/v) and 1.7 ± 0.4 AuNPs (0.002% w/v) was heated to 60 °C to dissociate BHPB and cooled to room temperature to reassemble it in the presence of AuNPs. This mixture was allowed to stabilize overnight before drop-casting on TEM grids for observation. It turned out that the nanotape morphology in the hybrids obtained in this fashion is different from that observed for hybrids obtained by the mixing method (Figure 4a,b and Supporting Information, Figure S5). In samples prepared by the heat/cool method, the nanotapes were largely coiled and far less ordered/bundled, implying that the presence of AuNPs during nanotape formation affects template assembly. AuNPs were distributed regularly along the rims of these coiled tapes (Figure 4b). As the infrared spectra of the hybrid obtained from heat/cool method was identical to that of native BHPB nanosheets (Supporting Information, Figure S6), it can be concluded that the presence of AuNPs does not affect

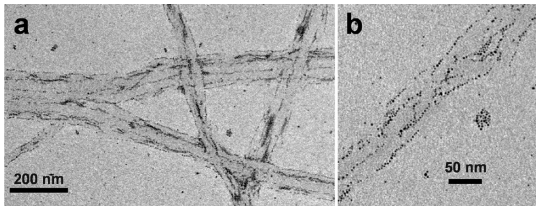

Figure 4. TEM images of AuNP–BHPB hybrids obtained by the heat/cool method. The sol obtained by heating 1.7 ± 0.4 nm dodecanethiol–AuNPs (0.002% w/v) and self-assembled BHPB (0.02% w/v) was stabilized overnight before drop casting on TEM grids.

the primary assembly mechanism of the BHPB molecules. It appears that the association of AuNPs with BHPB and its primary aggregates competes with the secondary assembly mechanism of BHPB; that is, the formation of nanosheets and the latter is largely suppressed. Perhaps, the internanotape association (nanosheet formation) stabilizes the planar structure of the nanotapes and in its absence, the nanotapes tend to coil. Thus, the heat/cool method suffers from the disadvantage of template structure alteration, and, under heating conditions, Oswald ripening of AuNPs can take place.[25] Consequently, this method of AuNP organization cannot be considered as an ideal template-assisted assembly process.

To understand the organization process, self-assembly of BHPB and its association with AuNPs were studied by UV–vis spectroscopy. Shown in Figure 5 are the UV–vis spectra of BHPB in the associated (nanotape suspension) and dissociated states (sol) and its hybrid with AuNPs obtained by (i) mixing and (ii) heat/cool. In the sol state, BHPB (0.02% w/v) in cyclohexane shows absorption bands at 250 and 305 nm. Upon assembly, the bands broaden and a new band at 268 nm appears (Figure 5 and Supporting Information, Figure S7a). The intensities of the two bands are decreased as a result of this broadening. These changes are consistent with $\pi-\pi$ stacking interactions of the benzene cores during assembly.[32] Upon being mixed with AuNPs (0.002% w/v), the spectral band intensities are proportionally enhanced (Figure 5 and Supporting Information, Figure S7b). That is, the absorption cross-section of the self-assembled BHPB molecules is increased due to metal enhanced electromagnetic fields,[35,36] suggesting its association with AuNPs. When the hybrid is heated to dissociate the BHPB molecules, the spectral bands of the sol reappeared with increased intensities. This implies that the AuNPs remain associated with the BHPB molecules and its aggregates present in the sol. Upon cooling this sol to room temperature to allow BHPB to self-assemble, the band centered at 260 nm appeared with the same intensity as that of the hybrid obtained by the mixing method, whereas the band at 310 nm exhibited higher intensity. Notably, the intensity of this band is equivalent to that of the sol. That is, the assembly of BHPB in

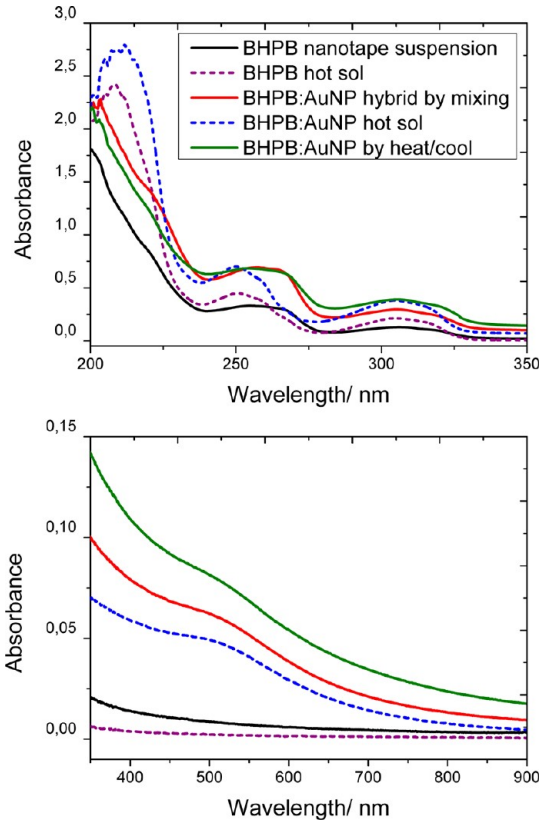

Figure 5. UV–vis spectra of self-assembled suspensions and sols of BHPB (0.02% w/v) and its hybrids with AuNPs (0.004% w/v), prepared by mixing and heat/cool methods. Spectral bands for BHPB absorption are shown on top and the AuNP plasmon band range is enlarged and shown separately at the bottom. Complete spectra are shown in Supporting Information, Figure S7b.

the presence of AuNPs is not identical to that of native BHPB nanotapes. Comparing this with the TEM results where the nanotapes obtained in the presence of AuNPs were found to be coiled indicates that the changed 310 nm band intensity is related to this process.

For hybrids prepared by either of the methods, the AuNP plasmon band position did not show any detectable spectral shift as compared to the plasmon band in the sol state (Figure 5) or the cyclohexane dispersion of AuNPs. The intensities of the plasmon bands were however different for the two hybrids and the sol of the hybrid, owing to the differential light scattering properties of the three mixtures.

Both UV–vis results and characteristic features of the NP arrays observed in TEM suggest that the association of the AuNPs with the templates happened most likely in suspensions. The absence of plasmon band shift for the hybrids does not necessarily imply that the assembly of AuNPs does not occur in suspension because theoretically the plasmon resonance decays exponentially over ~20% of the AuNP core size and hardly any plasmon coupling and hence spectral shift is expected for 1.7 ± 0.4 nm sized AuNPs

separated by 1.7−2.5 nm interparticle distances.[37,38] This was verified by measuring the absorption spectra of a coffee ring pattern obtained by evaporative self-assembly[39] of a drop of 1.7 ± 0.4 nm AuNPs on APTMS coated glass slide. The absorption spectrum of the solid coffee ring constituting a close-packed assembly of AuNPs was similar to that of a AuNP dispersion in cyclohexane (Supporting Information, Figure S7c), confirming the absence of plasmon coupling for assemblies of these particles. The hypothesis was further confirmed by a control TEM sample. Apparently, regular arrays of AuNPs could not be obtained by sequential deposition of equal volumes (10 μL) of 0.02% w/v BHPB suspension and 0.002% w/v dispersion of dodecanethiol AuNPs in cyclohexane (Supporting Information, Figure S8). In samples prepared in this fashion, AuNPs accumulated into patches along the step edges formed by the template on the supporting carbon surface and did not align along the template valleys and edges to produce linear arrays. In light of this, it is reasonable to conclude that the observed homogeneous organization of AuNP on the BHPB template in samples obtained by the mixing method is unlikely to have occurred during TEM grid preparation.

Thus, self-assembled BHPB serves as an excellent template for the organization of 1.7 nm sized dodecanethiol stabilized AuNP. It is noteworthy that the periodic 1D organization of AuNPs achieved using the BHPB template is comparable to the ones obtained using programmed, self-assembled DNA tiles.[14] These assemblies are also comparable to assemblies obtained with phase separating block copolymers.[15] Organizational order obtained with the BHPB template is the best when compared to those achieved so far using other self-assembled synthetic small molecule templates. Some of the previous approaches for organizing NPs on self-assembled fibers consisted of using thiol anchoring[21−23] or H-bonding[24] to facilitate binding of the NPs to the self-assembled fibers. This necessitated the presence of thiol groups or H-bonding units in the self-assembling molecule/nanoparticle surface, which were incorporated through additional synthetic procedures to prepare thiol analogues and nanoparticle surface modification. Such procedures are not required in our strategy because specific interaction was not required for AuNP organization on the template. All the previous approaches[20−30] also use high concentrations of self-assembling molecules to obtain solid gel samples comprising a dense entangled network of fibers decorated with gold NPs. These solid assemblies have limited applicability.[40] On the contrary, assemblies constructed using suspensions of self-assembled BHPB molecules offer the distinct advantage of easy transferability to different substrates.

Using the clues provided by spectral and TEM results, a model for the self-assembly of BHPB and its association with AuNP is proposed (Figure 6). In its

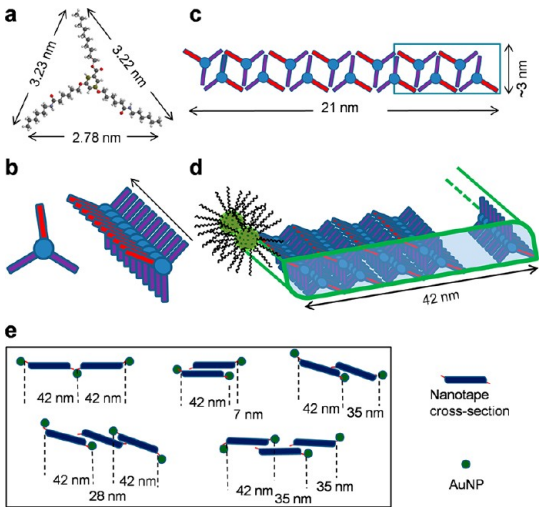

Figure 6. Schematics of BHPB assembly and the association of BHPB nanosheets with AuNPs: (a) energy minimized structure of BHPB; (b) cartoon of BHPB, in which red bar corresponds to ester arm and molecular packing along the fiber length, involving $\pi-\pi$ interaction of the benzene core and intermolecular H-bonding between the amide linkages of the side arms. Arrow points at the H-bonding direction; (c) molecular arrangement along the width of the nanotape with a box showing 7 nm repeating unit; (d) complete picture of the arrangement showing BHPB molecules projecting an alkyl group array at the tape edges and the association of gold NPs through interdigitation; (e) cross-sectional view of possible ways in which 2−3 nanotapes can be organized in a nanosheet. Assigning a nanoparticle to each extremity and one to an overlap yields inter NP-stripe distances of 42, 35, 28, and 7 nm measured on TEM.

minimum energy conformation, BHPB is a Y-shaped molecule with two of its edge lengths equal to 3.2 nm each and the remaining equal to 2.7 nm. UV−vis and infrared spectral studies (Supporting Information, Figures S6 and S7a)[32] indicate that BHPB molecules associate through the $\pi-\pi$ interaction of the benzene cores and the intermolecular H-bonding interaction between the amide linkages of the side arms. It is reasonable to assign these interactions to the favored growth axis, which corresponds to the nanotape length (Figure 6b). The BHPB nanosheet suspensions did not yield any diffraction signals owing to their low concentration and also lack of long-range order. Shown in Figure 6c,d is a possible molecular packing of BHPB in the nanotape, consistent with the observed structural parameters. Other possible molecular arrangements and the reason for choosing this particular model are discussed in the Supporting Information (Figure S9). As the AuNPs do not bind to the template through specific interaction (no IR spectral shift for the hybrid as compared to native BHPB nanosheet (Figure S6)), it is reasonable to assume that the gold NPs associate with BHPB template through van der Waals interaction.[41] This attractive interaction most likely arises from the interdigitation of the dodecanethiol molecules capping the nanoparticles with the ester alkyl arms of BHPB (which are of same length), projected from the

nanotape edges, as shown in Figure 6d. The model for the organization of the nanotapes into nanosheets to generate the measured inter NP-stripe distances is shown in Figure 6e. In this model, BHPB nanotapes are considered to project arrays of alkyl groups at their edges, in diametrically opposite direction and run antiparallel with respect to their immediate neighbor. Two nanotapes can organize in three ways: (i) laterally without overlap, (ii) laterally with 7 nm overlap or (iii) face to face with a 7 nm offset. Typically, overlap of two nanotapes creates two valleys (one on each face of the formed nanosheet), but only one of these valleys has an alkyl array projected outward, and AuNPs are preferentially attached to this face. Using this model, inter NP-stripe distances measured on nanosheets consisting of mono- and bilayered nanosheets made of several nanotapes can easily be explained.

Apparently, the organized AuNPs function as staining agents and provide a good contrast for obtaining structural information about BHPB superstructures and their ordering. A similar observation was made in the recent past by Pradeep *et al.*, who used AuNPs to probe the preliminary stages of the self-assembly of oligo(*p*-phenylenevinylene)-derivatives.[42] The information about the nanotape organization into a nanosheet obtained from gold NP organization is almost impossible to obtain from platinum-stained TEM images which present unclear contrast. Evidently, such strategies may be more generally adopted as complementary tools to obtain deeper insights into various structural features of self-assembled systems.

AuNP Size-Selection and Size-Sorting. Encouraged by the success of assembling small gold NPs, attempts were made to organize bigger 5.4 ± 1.0 nm sized dodecanethiol stabilized AuNPs. A TEM of mixtures of BHPB and larger AuNPs indicated that the templates failed to order these NPs into 1D array. The 5.4 nm sized AuNPs were either randomly attached to the nanotapes/nanosheets or aligned along their external edges, as observed in some regions of the TEM. Very few particles were found in the inner valleys (as shown in Figure 7a and Supporting Information, Figure S10a). This means, the 5.4 ± 1.0 nm AuNPs are too large to be able to dock onto the valleys. In other words, the inner valleys of the template impose a geometric restriction on the organized NPs. Results similar to this have been reported by Teranishi *et al.* for the organization of dodecanethiol-protected gold nanoparticles on ridge-and-valley structured carbon (hard template), whose dimensions are comparable to that of self-assembled BHPB structures. They have shown that 3.4 nm AuNPs organize better on nanostructured carbon than the larger 5.4 nm ones.[43]

UV−vis spectra of these hybrids showed increased absorption as compared to a native BHPB nanosheet suspension, which can be attributed to increased electromagnetic fields around the chromophores

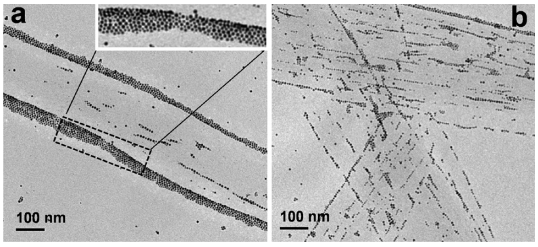

Figure 7. TEM images showing AuNP organization achieved from a mixture of self-assembled nanosheets of BHPB (0.02% w/v) in cyclohexane and 5.4 ± 1.0 nm dodecanethiol−AuNPs by (a) mixing and (b) sonicating. The inset in panel a shows an enlarged view of the organized NPs.

owing to the proximity of the AuNPs to the BHPB nanosheets (Supporting Information, Figure S10b). However, no detectable plasmon resonance shift was observed. On the other hand, a coffee ring[39] formed on an APTMS-coated glass slide using these particles yields a spectral shift of ~20 nm (Figure S10c).[38] The fact that no plasmon band shift was detected for the BHPB:AuNP hybrids implies that the association of AuNPs with the template has not occurred to a significant extent in the liquid phase. The nonhomogeneity of the organization observed in TEM and AuNP alignment mainly along the template edges also indicates that most of the observed linear organization results from solvent drying effects. The presence of multiple layers of AuNPs at the external edges (shown in the inset of Figure 7a) supports this argument. It is also possible that the AuNPs are attached randomly to the nanosheet bundles or organized only on the edges of multiply stacked thicker nanosheets, the population of which might not be large enough to alter the absorption spectra.

Sonicating mixtures of BHPB and 5.4 ± 1.0 nm AuNPs briefly on an ultrasonic cleaner before dropcasting on TEM grids increased the number of AuNPs in the inner valleys, as noticed in some sections of the TEM images (Figure 7b). UV−vis spectra of these samples did not show an observable shift in surface plasmon resonance (Supporting Information, Figure S11), making it difficult to predict if the organization occurred in the liquid phase. Nevertheless, sonication could not be considered as a suitable method for obtaining such assemblies, as it considerably altered the soft templates (Supporting Information, Figure S12). Under sonication, severe bundling and shortening of templates was observed. It is possible that the sonication creates step-edges in the nanosheet bundles, and the organization observed in TEM is a result of solvent drying mediated assembly along these structural features.

Thus, the BHPB nanosheets fail to organize 5.4 ± 1.0 nm AuNPs in a manner similar to 1.7 ± 0.4 nm AuNPs. Given these observations, it appeared that selective assembly of smaller NPs in the inner valleys even in the presence of bigger ones may be achieved.

When a mixture of 1.7 ± 0.4 nm and 5.4 ± 1.0 nm AuNPs was used for generating assemblies, AuNPs organized into stripes consisted largely of smaller ones (Figure 8 and Supporting Information, Figure S13). Only a few of the bigger AuNPs were located on the external edges of the array with most of them remaining in regions outside these arrays. The results clearly suggest that the inner valleys of the nanosheet essentially select smaller nanoparticles. On the other hand, template edges appear to show less specificity to NP size: both small and large particles were found to be attached at the edges. The observed characteristics supports the idea that the association of small AuNPs with the template takes place in the liquid phase while the larger AuNPs align along the template edges and step-edge features present on nanosheets due to solvent drying effects, during TEM sample preparation.

Interestingly, when gold NPs of average size 2.5 nm with a broad Gaussian size distribution (2.5 ± 0.9 nm) was used for organization, occurrence of size-selection was clearly evident (Supporting Information, Figure S14a). In TEM images of these assemblies, the NPs forming straight arrays are smaller in size than those remaining outside. The latter formed a random network. Analysis of the TEM images of the assembly also revealed size-sorting of the AuNPs associated with the template. Size analysis carried out over 1000 NPs indicated that the AuNPs organized along the inner valleys are 1.6 ± 0.8 nm in size, while those attached to the edges are larger. For instance, in the planar array shown in Figure 9a, the sizes of the NPs along the inner valleys and outer edges are 1.6 ± 0.6 and, 3.1 ± 1.2, respectively. The coiling tape crossing this array is not considered in the size analysis. Because this array shows the presence of more than one layer of NPs at the external edges, suggesting their accumulation due to solvent drying effects, a similar analysis was carried out on another array shown in Figure 9b, where such effect seemed to be minimal. In this case, the inner valleys once again contained NPs of sizes 1.6 ± 0.8 nm while those on the outer edges were 2.2 ± 0.9 nm in size. The size-sorting feature demonstrated in Figures 9a,b was observed throughout the sample (other representative images are shown in Figure S14b), and this unequivocally suggests that the ordering of ~2 nm AuNPs occurs in the liquid phase rather than on the TEM grid.

The observed size-sorting behavior indicates that the BHPB template is sensitive to a very narrow difference in the NP size. The phenomena of size-sorting are often observed with nanosized objects[44,45] and the particular case presented here is induced by the template topography. The size selectivity exhibited in this assembly is most likely a result of complementarities of the shape and the dimension of the nanovalleys with that of the associated gold nanoparticles (1.6 ± 0.8 nm). This has similarities to a typical lock-and-key type assembly process[46,47] and may very well be driven by entropy.[41,48−50] Further experiments and theoretical studies are planned to understand the nature of forces driving this organization.

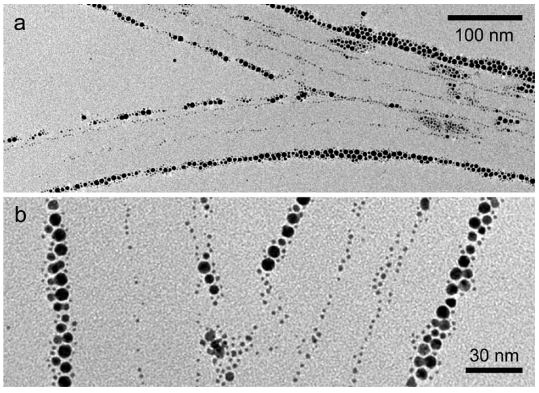

Figure 8. (a) TEM image of gold NP array obtained using a mixture of BHPB nanosheets (0.02% w/v) in cyclohexane and dodecanethiol−AuNPs of sizes 5.4 ± 1.0 nm and 1.7 ± 0.4 nm. (b) Enlarged image of the middle part of the array exhibiting a typical size-sorting effect.

CONCLUSIONS

A simple method to organize readily available 2 nm sized dodecanethiol capped AuNPs into periodic 1D

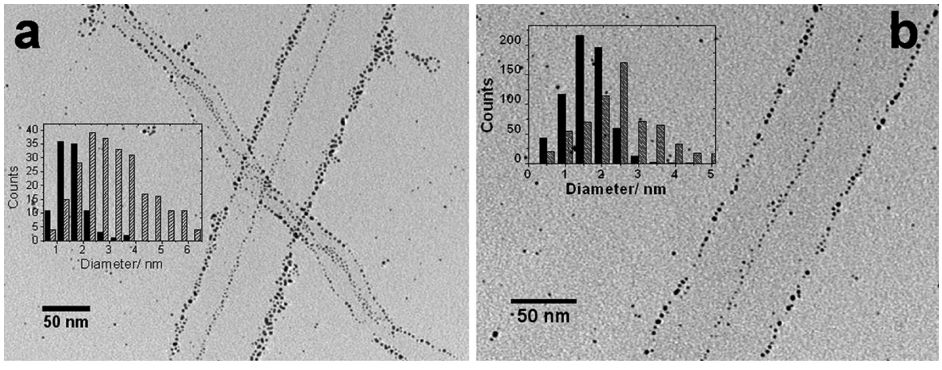

Figure 9. TEM images of size-sorted gold NP arrays obtained using a mixture of BHPB nanosheets (0.02% w/v) in cyclohexane and dodecanethiol−AuNP of size 2.5 ± 0.9 nm. Insets show the AuNP size distributions in the inner valley (black bar) and external edges (gray bar) of the template.

arrays by making use of surface topographical features of hierarchically organized BHPB soft templates is described. The organization achieved with BHPB templates using nonspecific van der Waals interactions is comparable to those obtained using programmed DNA[14] and block copolymer templates,[15] where the two associating components, template, and the nanoparticles were tailored to interact specifically.

The observed AuNP organization on the BHPB template appears to be driven by entropy *via* a lock-and-key type mechanism, with the BHPB template acting as lock and AuNPs fitting in as keys. While the template spontaneously organizes AuNPs of approximately 2 nm size, it failed to yield similar results for the larger 5.4 nm sized NPs. This indicates that the size complementarity of the associating components (BHPB template and AuNP) is a determinant factor in the organization process. Valleys present on BHPB nanosheets imposed steric restrictions on the assembled AuNPs and led to the preferential association of AuNPs of size 1.6 ± 0.8 nm when a polydisperse sample (2.5 ± 0.9 nm) was used for organization. As template edges did not present such geometric constraints, size-sorted assemblies were obtained. Such size-sorting effects can have significant implications in building NP assemblies. Besides, the size selection property of the BHPB nanosheets offers the possibility of using such materials as membranes for size fractionation of NPs.[51]

The organization strategy described here can be readily extended to a variety of NP cores (metal, magnetic, semiconductor) protected with simple alkyl ligands. Given the vast diversity of self-assembling molecules,[52] a combination of the two can lead to materials with interesting properties and applications. Furthermore, NP assemblies obtained using our template may readily be transferred to different desired substrates and possibly aligned in preferred directions. Such maneuverability is essential for processing solution based assemblies into devices.

METHODS

BHPB was synthesized as previously described.[32] Gold NPs were synthesized following literature procedures.[33] The experimental procedures and TEM images of the nanoparticles along with their size distribution plots are included in the Supporting Information (Figure S15–S17).

Preparation of BHPB Nanotapes (0.02% w/v). A 2 mg portion of BHPB was heated with 10 mL of cyclohexane in a tightly capped glass vial to obtain a homogeneous solution and then cooled to room temperature (RT) under ambient conditions. A cloudy suspension of BHPB nanotapes was obtained in about 5–10 min. This was left undisturbed at RT for about 12 h before use.

Preparation of BHPB-AuNP Hybrids. The organization of ~2 nm sized AuNPs by mixing method was achieved by shaking 1 mL of BHPB nanotape suspension in cyclohexane (0.02% w/v) and a known volume (typically between 10 and 20 μL) of 2 mg/mL AuNP dispersion in cyclohexane in a tightly capped 4 mL volume glass vial and leaving the resulting brown colored mixture undisturbed overnight at RT. The mixture was then drop-casted on carbon coated copper grid for TEM observations. For obtaining assemblies with larger 5.4 ± 1.0 AuNPs, 10–20 μL of 6 mg/mL dispersion in cyclohexane were used. For obtaining assemblies with the small and large AuNPs mixture, 10 μL of 2 mg/mL dispersion of 1.7 ± 0.4 nm AuNPs and 10 μL of 2 mg/mL dispersion of 5.4 ± 1.0 nm AuNPs in cyclohexane were used.

For preparing hybrids by the heat/cool method, the same quantities of the template suspension and nanoparticle dispersions were used. The tightly capped glass vial containing the mixtures were heated to ~60 °C to obtain a clear pale brown solution and incubated overnight at RT.

Transmission Electron Microscopy (TEM). BHPB nanosheet suspensions and BHPB–AuNP hybrids were dropcasted on carbon-coated copper grids held in contact with filter paper to enable quick draining and drying of the sample. The sample was dried further under ambient conditions. Whereas the BHPB nanotape samples were shadowed with Pt before TEM observations, the BHPB–AuNP hybrids were observed as such without staining, using a Philips CM12 microscope operating at 120 kV.

Atomic Force Microscopy (AFM). The BHPB nanotape suspension (0.02% w/v) was diluted five times by the addition of cyclohexane and a drop of the resulting suspension was dried on freshly cleaved mica under ambient conditions. AFM measurements were done with a Multimode AFM and Nanoscope IV controller from Veeco (Santa Barbara, CA), in tapping mode under ambient conditions (air and room temperature). Cantilevers with a nominal resonant frequency of 300 kHz and a typical spring constant of 40 N/m were used. Tips are made of silicon with terminal tip radius less than 10 nm. We always performed several scans over a given surface area. These scans had to produce comparable images to indicate that there was no sample damage induced by the tip. Images were scanned at different scales at a fixed scan rate of 1 Hz with a resolution of 512×512 pixels.

UV–vis Spectroscopy. UV–vis spectra were recorded on Perkin-Elmer Lambda 35 spectrometer. A 4 mm path length quartz cell was used for all the measurements. Typically, a hot sol of the BHPB in cyclohexane was transferred to the cell and allowed to self-assemble by letting stand at RT overnight before recording the absorption spectra. For preparing hybrid, an appropriate quantity of the AuNP dispersion in cyclohexane was added to this mixture and shaken.

Conflict of Interest: The authors declare no competing financial interest.

Acknowledgment. This project was supported by the International Center for Frontier Research in Chemistry, Strasbourg. Mark Schmutz is acknowledged for help with TEM. Sangeetha N. M. acknowledges CNRS for a Poste Rouge.

Supporting Information Available: AFM images of the template, electron micrographs of BHPB:AuNP hybrids, UV–vis and IR spectra of BHPB and its hybrid with AuNPs, experimental procedures for the synthesis of the dodecanethiol stabilized gold nanoparticles. This material is available free of charge via the Internet at http://pubs.acs.org.

REFERENCES AND NOTES

1. Shipway, A. N.; Katz, E.; Willner, I. Nanoparticle Arrays on Surfaces for Electronic, Optical, and Sensor Applications. *Chem. Phys. Chem.* **2000**, *1*, 18–52.
2. Katz, E.; Willner, I. Integrated Nanoparticle–Biomolecule Hybrid Systems: Synthesis, Properties, and Applications. *Angew. Chem., Int. Ed.* **2004**, *43*, 6042–6108.
3. Nie, Z.; Petukhova, A.; Kumacheva, E. Properties and Emerging Applications of Self-Assembled Structures Made from Inorganic Nanoparticles. *Nat. Nanotechnol.* **2010**, *5*, 15–25.

4. Tan, S. J.; Campolongo, M. J.; Luo, D.; Cheng, W. Building Plasmonic Nanostructures with DNA. *Nat. Nanotechnol.* **2011**, *6*, 268–276.
5. Gates, B. D.; Xu, Q.; Stewart, M.; Ryan, D.; Willson, C. G.; Whitesides, G. M. New Approaches to Nanofabrication: Molding, Printing, and Other Techniques. *Chem. Rev.* **2005**, *105*, 1171–1196.
6. Koh, S. J. Strategies for Controlled Placement of Nanoscale Building Blocks. *Nanoscale Res. Lett.* **2007**, *2*, 519–545.
7. Mann, S. Self-Assembly and Transformation of Hybrid Nano-objects and Nanostructures under Equilibrium and Non-equilibrium Conditions. *Nat. Mater.* **2009**, *8*, 781–792.
8. Grzelczak, M.; Vermant, J.; Furst, E. M.; Liz-Marzán, L. M. Directed Self-Assembly of Nanoparticles. *ACS Nano* **2010**, *4*, 3591–3605.
9. Niemeyer, C. M. Nanoparticles, Proteins, and Nucleic Acids: Biotechnology Meets Materials Science. *Angew. Chem., Int. Ed.* **2001**, *40*, 4128–4158.
10. Mirkin, C. M.; Letsinger, R. L.; Mucic, R. C.; Storhoff, J. J. A DNA-Based Method for Rationally Assembling Nanoparticles into Macroscopic Materials. *Nature* **1996**, *382*, 607–609.
11. Aldaye, F. A.; Sleiman, H. F. Dynamic DNA Templates for Discrete Gold Nanoparticle Assemblies: Control of Geometry, Modularity, Write/Erase and Structural Switching. *J. Am. Chem. Soc.* **2007**, *129*, 4130–4131.
12. Wang, Z.; Lévy, R.; Fernig, D. G.; Brust, M. The Peptide Route to Multifunctional Gold Nanoparticles. *Bioconjugate Chem.* **2005**, *16*, 497–500.
13. Zheng, J.; Constantinou, P. E.; Micheel, C.; Alivisatos, A. P.; Kiehl, R. A.; Seeman, N. C. Two-Dimensional Nanoparticle Arrays Show the Organizational Power of Robust DNA Motifs. *Nano Lett.* **2006**, *6*, 1502–1504.
14. Sharma, J.; Ke, Y.; Lin, C.; Chhabra, R.; Wang, Q.; Nangreave, J.; Liu, Y.; Yan, H. DNA-Tile-Directed Self-Assembly of Quantum Dots into Two-Dimensional Nanopatterns. *Angew. Chem., Int. Ed.* **2008**, *120*, 5235–5237.
15. Shenhar, R.; Norsten, T. B.; Rotello, V. M. Polymer-Mediated Nanoparticle Assembly: Structural Control and Applications. *Adv. Mater.* **2005**, *17*, 657–669.
16. Lin, Y.; Böker, A.; He, J.; Sill, K.; Xiang, H.; Abetz, C.; Li, X.; Wang, J.; Emrick, T.; Long, S.; *et al.* Self-Directed Self-Assembly of Nanoparticle/Copolymer Mixtures. *Nature* **2005**, *434*, 55–59.
17. Bockstaller, M. R.; Lapetnikov, Y.; Margel, S.; Thomas, E. L. Size-Selective Organization of Enthalpic Compatibilized Nanocrystals in Ternary Block Copolymer/Particle Mixtures. *J. Am. Chem. Soc.* **2003**, *125*, 5276–5277.
18. Zhao, Y.; Thorkelsson, K.; Mastroianni, A. J.; Schilling, T.; Luther, J. M.; Rancatore, B. J.; Matsunaga, K.; Hiroshi, J.; Wu, Y.; Poulsen, D.; *et al.* Small-Molecule-Directed Nanoparticle Assembly Towards Stimuli-Responsive Nanocomposites. *Nat. Mater.* **2009**, *8*, 979–985.
19. Sangeetha, N. M.; Maitra, U. Supramolecular Gels: Functions and Uses. *Chem. Soc. Rev.* **2005**, *34*, 821–836.
20. Simmons, B.; Li, S.; John, V. T.; McPherson, G. L.; Taylor, C.; Schwartz, D. K.; Maskos, K. Spatial Compartmentalization of Nanoparticles into Strands of a Self-Assembled Organogel. *Nano Lett.* **2002**, *2*, 1037–1042.
21. Kimura, M.; Kobayashi, S.; Kuroda, T.; Hanabusa, K.; Shirai, H. Assembly of Gold Nanoparticles into Fibrous Aggregates Using Thiol-Terminated Gelators. *Adv. Mater.* **2004**, *16*, 335–338.
22. van Herrikhuyzen, J.; George, S. J.; Vos, M. R. J.; Sommerdijk, N. A. J. M.; Ajayaghosh, A.; Meskers, S. C. J.; Schenning, A. P. H. J. Self-Assembled Hybrid Oligo(p-phenylenevinylene)–Gold Nanoparticle Tapes. *Angew. Chem., Int. Ed.* **2007**, *46*, 1825–1828.
23. Bose, P. P.; Drew, M. G.B.; Banerjee, A. Decoration of Au and Ag Nanoparticles on Self-Assembling Pseudopeptide-Based Nanofiber by Using a Short Peptide as Capping Agent for Metal Nanoparticles. *Org. Lett.* **2007**, *9*, 2489–2492.
24. Puigmartí-Luis, J.; del Pino, Á.P.; Laukhina, E.; Esquena, J.; Laukhin, V.; Rovira, C.; Vidal-Gancedo, J.; Kanaras, A. G.; Nichols, R. J.; Brust, M.; *et al.* Shaping Supramolecular Nanofibers with Nanoparticles Forming Complementary Hydrogen Bonds. *Angew. Chem., Int. Ed.* **2008**, *47*, 1861–1865.
25. Coates, I. A.; Smith, D. K. Hierarchical Assembly—Dynamic Gel-Nanoparticle Hybrid Soft Materials Based on Biologically Derived Building Blocks. *J. Mater. Chem.* **2010**, *20*, 6696–6702.
26. Bardelang, D.; Zaman, M. B.; Moudrakovski, I. L.; Pawsey, S.; Margeson, J. C.; Wang, D.; Wu, X.; Ripmeester, J. A.; Ratcliffe, C. I.; Yu, K. Interfacing Supramolecular Gels and Quantum Dots with Ultrasound: Smart Photoluminescent Dipeptide Gels. *Adv. Mater.* **2008**, *20*, 4517–4520.
27. Sangeetha, N. M.; Bhat, S.; Raffy, G.; Belin, C.; Loppinet-Serani, A.; Aymonier, C.; Terech, P.; Maitra, U.; Desvergne, J. P.; Del Guerzo, A. Hybrid Materials Combining Photoactive 2,3-DidecyloxyAnthracene Physical Gels and Gold Nanoparticles. *Chem. Mater.* **2009**, *21*, 3424–3432.
28. Li, L.-S.; Stupp, S. I. One-Dimensional Assembly of Lipophilic Inorganic Nanoparticles Templated by Peptide-Based Nanofibers with Binding Functionalities. *Angew. Chem., Int. Ed.* **2005**, *44*, 1833–1836.
29. Grzelczak, M.; Kulisic, N.; Prato, M.; Mateo-Alonso, A. Multimode Assembly of Phenanthroline Nanowires Decorated with Gold Nanoparticles. *Chem. Commun.* **2010**, 9122–9144.
30. Henry, E.; Dif, A.; Schmutz, M.; Legoff, L.; Amblard, F.; Marchi-Artzner, V.; Artzner, F. Crystallization of Fluorescent Quantum Dots within a Three-Dimensional Bio-organic Template of Actin Filaments and Lipid Membranes. *Nano Lett.* **2011**, *11*, 5443–5448.
31. Wang, Z.; Skirtach, A. G.; Xie, Y.; Liu, M.; Möhwald, H.; Gao, C. Core–Shell Poly(allyamine hydrochloride)–Pyrene Nanorods Decorated with Gold Nanoparticles. *Chem. Mater.* **2011**, *23*, 4741–4747.
32. Diaz, N.; Simon, X.-S.; Schmutz, M.; Rawiso, M.; Decher, G.; Jestin, J.; Mésini, P. J. Self-Assembled Diamide Nanotubes in Organic Solvents. *Angew. Chem., Int. Ed.* **2005**, *44*, 3260–3264.
33. Hostetler, M. J.; Wingate, J. E.; Zhong, C.-J.; Harris, J. E.; Vachet, R. W.; Clark, M. R.; Londono, J. D.; Green, S. J.; Stokes, J. J.; Wignall, G. D.; *et al.* Alkanethiolate Gold Cluster Molecules with Core Diameters from 1.5 to 5.2 nm: Core and Monolayer Properties as a Function of Core Size. *Langmuir* **1998**, *14*, 17–30.
34. Wang, Z. L.; Harfenist, S. A.; Whetten, R. L.; Bentley, J.; Evans, N. D. Bundling and Interdigitation of Adsorbed Thiolate Groups in Self-Assembled Nanocrystal Superlattices. *J. Phys. Chem. B* **1998**, *102*, 3078–3072.
35. Kühn, S.; Håkanson, U.; Rogobete, L.; Sandoghdar, V. Enhancement of Single-Molecule Fluorescence Using a Gold Nanoparticle as an Optical Nanoantenna. *Phys. Rev. Lett.* **2006**, *97*, 0174021–0174024.
36. Anger, P.; Bharadwaj, P.; Novotny, L. Enhancement and Quenching of Single-Molecule Fluorescence. *Phys. Rev. Lett.* **2006**, *96*, 1130021–1130024.
37. Jain, P. K.; Huang, W.; El-Sayed, M. A. On the Universal Scaling Behavior of the Distance Decay of Plasmon Coupling in Metal Nanoparticle Pairs: A Plasmon Ruler Equation. *Nano Lett.* **2007**, *7*, 2080–2088.
38. Chen, C.-F.; Tzeng, S.-D.; Chen, H.-Y.; Lin, K.-J.; Gwo, S. Tunable Plasmonic Response from Alkanethiolate-Stabilized Gold Nanoparticle Superlattices: Evidence of Near-Field Coupling. *J. Am. Chem. Soc.* **2007**, *130*, 824–826.
39. Han, W.; Lin, Z. Learning from "Coffee Rings": Ordered Structures Enabled by Controlled Evaporative Self-Assembly. *Angew. Chem., Int. Ed.* **2012**, *51*, 1534–1546.
40. Terech, P. Metastability and Sol Phases: Two Keys for the Future of Molecular Gels. *Langmuir* **2009**, *25*, 8370–8372.
41. Bishop, K. J. M.; Wilmer, C. E.; Soh, S.; Grzybowski, B. A. Nanoscale Forces and Their Uses in Self-Assembly. *Small* **2009**, *5*, 1600–1630.
42. Kumar, V. R. R.; Sajini, V.; Sreeprasad, T. S.; Praveen, V. K.; Ajayaghosh, A.; Pradeep, T. Probing the Initial Stages of Molecular Organization of Oligo(*p*-phenylenevinylene)

Assemblies with Monolayer Protected Gold Nanoparticles. *Chem. Asian J.* **2009**, *4*, 840–848.
43. Teranishi, T.; Sugawara, A.; Shimizu, T.; Miyake, M. Planar Array of 1D Gold Nanoparticles on Ridge-and-Valley Structured Carbon. *J. Am. Chem. Soc.* **2002**, *124*, 4210–4211.
44. Lee, J. S.; Stoeva, S. I.; Mirkin, C. A. DNA-Induced Size-Selective Separation of Mixtures of Gold Nanoparticles. *J. Am. Chem. Soc.* **2006**, *128*, 8899–8903.
45. Park, K.; Koerner, H.; Vaia, R. A. Depletion-Induced Shape and Size Selection of Gold Nanoparticles. *Nano Lett.* **2010**, *10*, 1433–1439.
46. Sacanna, S.; Irvine, W. T. M.; Chaikin, P. M.; Pine, D. J. Lock and Key Colloids. *Nature* **2010**, *464*, 575–578.
47. Macfarlane, R. J.; Mirkin, C. A. Colloidal Assembly *via* Shape Complementarity. *Chem. Phys. Chem.* **2010**, *11*, 3215–3217.
48. Adams, M.; Dogic, Z.; Keller, S. L.; Fraden, S. Entropically Driven Microphase Transitions in Mixtures of Colloidal Rods and Spheres. *Nature* **1998**, *393*, 349–352.
49. Lin, K.-h.; Crocker, J. C.; Prasad, V.; Schofield, A.; Weitz, D. A. Entropically Driven Colloidal Crystallization on Patterned Surfaces. *Phys. Rev. Lett.* **2000**, *85*, 1770–1773.
50. Dinsmore, A. D. Entropic Confinement of Colloidal Spheres in Corners on Silicon Substrates. *Langmuir* **1999**, *15*, 314–316.
51. Krieg, E.; Weissman, H.; Shirman, E.; Shimoni, E.; Rybtchinski, B. A Recyclable Supramolecular Membrane for Size-Selective Separation of Nanoparticles. *Nat. Nanotechnol.* **2011**, *6*, 141–146.
52. Terech, P.; Weiss, R. G. Low Molecular Mass Gelators of Organic Liquids and the Properties of Their Gels. *Chem. Rev.* **1997**, *97*, 3133–3160.